

Gene expression signatures and response to imatinib mesylate in gastrointestinal stromal tumor

Lori Rink,¹ Yuliya Skorobogatko,¹
 Andrew V. Kossenkov,¹ Martin G. Belinsky,¹
 Thomas Pajak,² Michael C. Heinrich,³
 Charles D. Blanke,⁴ Margaret von Mehren,¹
 Michael F. Ochs,⁵ Burton Eisenberg,⁶
 and Andrew K. Godwin¹

¹Department of Medical Oncology, Fox Chase Cancer Center, and ²Radiation Therapy Oncology Group, Philadelphia, Pennsylvania; ³Oregon Health and Science University, Portland, Oregon; ⁴University of British Columbia and the British Columbia Cancer Agency, Vancouver, British Columbia, Canada; ⁵The Sidney Kimmel Cancer Center, Johns Hopkins University, Baltimore, Maryland; and ⁶Norris Cotton Cancer Center, Dartmouth-Hitchcock Medical Center, Lebanon, New Hampshire

Abstract

Despite initial efficacy of imatinib mesylate in most gastrointestinal stromal tumor (GIST) patients, many experience primary/secondary drug resistance. Therefore, clinical management of GIST may benefit from further molecular characterization of tumors before and after imatinib mesylate treatment. As part of a recent phase II trial of neoadjuvant/adjuvant imatinib mesylate treatment for advanced primary and recurrent operable GISTs (Radiation Therapy Oncology Group S0132), gene expression profiling using oligonucleotide microarrays was done on tumor samples obtained before and after imatinib mesylate therapy. Patients were classified according to changes in tumor size after treatment based on computed tomography scan measurements. Gene profiling data were evaluated with Statistical Analysis of Microarrays to identify differentially expressed genes (in pretreatment GIST samples). Based

on Statistical Analysis of Microarrays [False Discovery Rate (FDR), 10%], 38 genes were expressed at significantly lower levels in the pretreatment biopsy samples from tumors that significantly responded to 8 to 12 weeks of imatinib mesylate, that is, >25% tumor reduction. Eighteen of these genes encoded Krüppel-associated box (KRAB) domain containing zinc finger (ZNF) transcriptional repressors. Importantly, 10 *KRAB-ZNF* genes mapped to a single locus on chromosome 19p, and a subset predicted likely response to imatinib mesylate-based therapy in a naïve panel of GIST. Furthermore, we found that modifying expression of genes within this predictive signature can enhance the sensitivity of GIST cells to imatinib mesylate. Using clinical pretreatment biopsy samples from a prospective neoadjuvant phase II trial, we have identified a gene signature that includes *KRAB-ZNF 91* subfamily members that may be both predictive of and functionally associated with likely response to short-term imatinib mesylate treatment. [Mol Cancer Ther 2009;8(8):2172–82]

Introduction

Gastrointestinal stromal tumors (GIST) are the most common mesenchymal tumors of the digestive tract, with between 3,300 to 6,000 new cases diagnosed each year in the United States (1). The most common primary sites for these neoplasms are the stomach (60–70%; refs. 2, 3), followed by the small intestine (25–35%; refs. 4, 5), and, to a much lesser degree, the colon and rectum (10%; ref. 6). GISTs have also been observed in the mesentery, omentum, esophagus, and the peritoneum (2, 7). GISTs occur most frequently in patients older than 50 years, with a median age of presentation of 58 years; however, GISTs have also been observed in the pediatric population (8). These tumors contain smooth muscle and neural elements, as described originally by Mazur and Clark in 1983, and are thought to arise from the interstitial cells of Cajal (9, 10). GISTs express and are clinically diagnosed by immunohistochemical (IHC) staining of the 145-kDa transmembrane glycoprotein, KIT, by the CD117 antibody. Most (~70%) GISTs possess gain-of-function mutations in *c-KIT* in either exons 9, 11, 13, or 17, causing constitutive activation of the kinase receptor, whereas smaller subsets of GISTs possess either gain-of-function mutations in *PDGFRA* (exons 12, 14, or 18; ~10%) or no mutations in either *KIT* or *PDGFRA* and are therefore referred to as wild-type GISTs (~15–20%; refs. 11–14). The primary treatment for GIST is surgical resection, which is often not curative in high risk GIST because of a high incidence of reoccurrence (15, 16). Since 2002, imatinib mesylate, an oral 2-phenylaminopyrimidine derivative that works as a selective inhibitor against mutant forms of type III tyrosine kinases, such as KIT, PDGFRA, and BCR/ABL, has become a standard treatment for patients with metastatic and/or

Received 12/3/08; revised 5/4/09; accepted 6/3/09; published OnlineFirst 8/11/09.

Grant support: NIH grants (CA106588 and a supplement from the Radiation Therapy Oncology Group to U10 CA21661; A.K. Godwin), LM009382 (M.F. Ochs), an award by the Fox Chase Cancer Center Translational Research Committee as part of the Fox Chase Cancer Center core grant (P30 CA006927; M. vonMehren and A.K. Godwin), and the NIH Training Grant (Institutional National Research Service Award Appointment (CA009035-31; L. Rink).

The costs of publication of this article were defrayed in part by the payment of page charges. This article must therefore be hereby marked *advertisement* in accordance with 18 U.S.C. Section 1734 solely to indicate this fact.

Note: L. Rink and Y. Skorobogatko contributed equally to this work. Current address for A.V. Kossenkov: Wistar Institute, Philadelphia, PA.

Requests for reprints: Andrew K. Godwin, Department of Medical Oncology, Fox Chase Cancer Center, 333 Cottman Avenue, Philadelphia, PA 19111. Phone: 215-728-2756; Fax: 215-728-2741. E-mail: Andrew.Godwin@fccc.edu

Copyright © 2009 American Association for Cancer Research.

doi:10.1158/1535-7163.MCT-09-0193

unresectable GIST, with objective responses or stable disease obtained in >80% of patients (17, 18). Response to imatinib mesylate has been correlated to the genotype of a given tumor (14). GIST patients with exon 11 *KIT* mutations have the best response and disease-free survival, whereas other *KIT* mutation types and wild-type GIST have worse prognoses. Despite the efficacy of imatinib mesylate, some patients experience primary and/or secondary resistance to the drug. ^{18}F -fluorodeoxyglucose-positron emission tomography can be used to rapidly assess tumor response to imatinib mesylate (19); however, there are cases in which GISTs do not take up significant amounts of the glucose precursor, and therefore, this scanning method is of questionable value in evaluating response in this group of patients. Strategies for treatment of progressive disease can include imatinib mesylate dose escalation (20), imatinib mesylate in combination with surgery, and alternative *KIT*/*PDGFRA* inhibitors, including sunitinib (21). There are also options to participate in clinical trials evaluating nilotinib (22), dasatinib (23), and HSP90 inhibitors (24). What may eventually prove to be the most effective paradigm in the clinical management of GIST is the development of individualized treatment approaches based on *KIT* and *PDGFRA* mutational status and/or predictive gene signatures of drug response. Ideally, in the future, patients may be preselected for treatment with imatinib mesylate or additional first- and second-line therapies based on these tumor-specific response markers.

The question of whether imatinib mesylate can be safe and effective as a rapid cytoreductive agent if administered before surgical resection has been evaluated in a recent novel phase II trial (Radiation Therapy Oncology Group Study 0132) of 8 to 12 weeks of neoadjuvant followed by adjuvant imatinib mesylate for either locally advanced primary or metastatic operable GIST. In this study, biopsies were taken at time of enrollment, and patients were treated with imatinib mesylate for 8 to 12 weeks before resection, followed by adjuvant imatinib mesylate treatment for 2 years. Contrast-enhanced computed tomography (CT) scans were done before, 4 to 6 weeks into treatment, and after the neoadjuvant imatinib mesylate regimen to document classic tumor response by response evaluation criteria in solid tumors (RECIST). Based on CT response data, patients for this study were classified in to two groups, group A (defined as $\geq 25\%$ tumor shrinkage after 8–12 weeks of imatinib mesylate) and group B (<25% tumor shrinkage, unchanged, or evidence of tumor enlargement after 8–12 weeks of imatinib mesylate). Microarray analysis of pretreatment GIST biopsies identified a gene signature of 38 response genes. These included Krüppel-associated box (KRAB)-zinc finger (ZNF) genes that were significantly expressed in tumor biopsies from patients less responsive to short-term treatment of imatinib.

Materials and Methods

Patient Selection

Sixty-three patients (52 analyzable) with primary or recurrent operable GIST were enrolled onto the Radiation

Therapy Oncology Group S0132 trial from 18 institutions. Patients' GIST samples were screened for CD117 (*KIT*) positivity by standard IHC before participation in the clinical trial. Patients were required to have adequate hematologic, renal, and hepatic function, as well as measurable disease for response evaluation. All patients signed informed consent following Institutional Review Board approval for this study and were consented to provide baseline biopsies and operative tissue.

Collection of Samples

Tumor samples were obtained from pre-imatinib mesylate core needle biopsies (pretreatment samples) and from the surgical specimen obtained at the time of resection following neoadjuvant/preoperative imatinib mesylate (posttreatment samples). A total of 48 pre- and 34 post-imatinib-treated samples were collected and banked. All patients received imatinib mesylate at 600 mg daily by mouth, which was continued daily until the day of surgery, with dose modifications for protocol-defined toxicities. Fresh-frozen pre- and posttreatment GIST samples were collected from all participating institutions and shipped to the Radiation Therapy Oncology Group tissue bank before evaluation.

RNA Isolation

Total RNA was isolated from all available pre- and post-frozen tissue samples using TRIzol reagent, according to the protocols provided by the manufacturer (Invitrogen Corp.). RNA quantification and quality assessment were done on 2100 Bioanalyser (Agilent Technologies). Because of the high variability in tissue collection and handling, storage and shipping procedures among the 18 institutions involved in the study, and the tumor cellularity of the specimens, 35% (17 of 48) of pre- and 26% (9 of 34) of posttreatment samples were of limited quality and were therefore excluded from the gene profiling studies. Furthermore, one of the samples was excluded because the CT response data were lacking.

DNA Isolation

Genomic DNA was isolated as previously described (25). Quality DNA was isolated from 38 cases (2 pretreatment biopsies and 36 posttreatment samples) and used for mutational analyses.

KIT and *PDGFRA* Mutational Status Analysis

Mutational analysis was done as previously described (26).

RNA Amplification and Microarray Hybridization

Fifty nanograms of RNA from the various tissue samples as well as 50 ng of Universal Human Reference RNA (Stratagene) were amplified using Ovation Aminoallyl RNA amplification and labeling system (NuGEN Technologies, Inc.). Aminoallyl cDNA was purified with QIAquick PCR Purification Kit (Qiagen), and yield was measured using Spectrophotometer ND-1000 (NanoDrop). Sample aminoallyl cDNA was labeled with Alexa Fluor 647 dye (Invitrogen Corp.), and reference aminoallyl cDNA was labeled with Alexa Fluor 555 dye (Invitrogen) as follows. Content of one vial from Alexa Fluor Reactive Dye Decapacks for Microarray Applications (Invitrogen) was resuspended in 2.5 μL of DMSO (Clontech) and added to 2 mg of aminoallyl cDNA, which was previously dried down in

vacuum centrifuge and resuspended in 7.5 μ L of coupling buffer (66.5 mmol/L NaHCO₃; pH 9.0). After incubation for 1 h in darkness at room temperature, reaction was purified with QIAquick PCR Purification Kit (Qiagen). Labeling efficiency was assessed on Spectrophotometer ND-1000 (NanoDrop). Labeled sample and reference were combined and hybridized on 44K Whole Human Genome Oligo Microarray (Agilent) at 60°C for 17 h. Washing was done in 6 \times saline-sodium phosphate-EDTA buffer with 0.005% Sarcosine at room temperature for 1 min; 0.06 \times saline-sodium phosphate-EDTA buffer with 0.005% Sarcosine at room temperature for 1 min, and then treated with Agilent Stabilization and Drying Solution at room temperature for 30 s.

Data Analysis

For the microarray studies, we were able to obtain high quality RNA and array data from 28 pretreatment samples and 25 posttreatment samples. For 17, we had matching pairs. Amplified and labeled RNAs were competitively hybridized against Stratagene Human Reference RNA using Agilent 4112a Whole Genome Human microarrays, scanned with an Agilent GMS 428 scanner, and preprocessed using the Functional Genomics Data Pipeline (27). These arrays were checked for quality by Agilent quality control and by visual inspection of MA plots pre- and post-LOESS normalization (width, 0.7; no background correction). Arrays that were of poor quality (i.e., which showed signs of RNA degradation such as splitting of MA plots into two “wings”) were repeated on a second RNA isolation from the same biopsy or tumor sample.

Clinical RECIST response is typically defined as a 30% decrease in the longest tumor diameter in the case of a primary target lesion or the sum of the longest diameters in the case of index tumors of metastatic disease. For the purpose of this analysis, as surgery occurred at a median of 65 d from the start of imatinib mesylate therapy, we arbitrarily divided these patients into group A (\geq 25% tumor shrinkage after 8–12 wk of imatinib mesylate) or group B ($<$ 25% tumor shrinkage, unchanged, or evidence of tumor enlargement after 8–12 wk of imatinib mesylate). In the seminal phase II metastatic GIST study, the median time to partial response (\geq 30% reduction) was 16 wk; therefore, we concluded that the duration of preoperative imatinib mesylate was probably too short to expect a significant number of patients having a classic partial response per RECIST. We therefore chose an arbitrary grouping of CT measured response for patients in group A of \geq 25% close to the 30% RECIST criteria for partial response. Had we selected \geq 30% decreased in tumor dimension, there would have been too few patients in group A for any meaningful analysis. All other patient's gene array samples that correlated clinically to \leq 25% decrease in tumor measurements, as determined by the study clinical parameters, were then placed in group B. It should be noted that gene profiling for predictive biomarkers of response was a post hoc analysis and not a primary or secondary endpoint of this original study. The 28 pretreatment samples were analyzed with Significance Analysis of Microarrays (28) implemen-

ted in the Multi-Experiment Viewer (29) to identify genes that showed significant pretreatment differential expression between the two groups. A false discovery rate of 10% was used. Microarrays were annotated using the most recent (August 20, 2007) Agilent annotation file. The most current accession number corresponding to Agilent IDs were retrieved from the file. Ensembl accession numbers were annotated with gene symbols and descriptions on June 6, 2008. Genebank accession numbers or gene names were annotated with National Center for Biotechnology Information Entrez information on June 9, 2008.

Because 10 of the differentially expressed genes mapped to the same locus (HSA19p12-19p13.1), we also analyzed all of the genes in this locus for response upon treatment (25 posttreatment samples, with 13 samples from group B and 12 from group A) with imatinib mesylate. We did this test by looking at each gene individually and looking for its average response in four categories: group A pretreatment, group B pretreatment, group A posttreatment, and group B posttreatment. Microarray data, including original Agilent scanner output files for all samples used in this study, are available through the Gene Expression Omnibus (accession number GSE15966).

Quantitative Reverse Transcription-PCR (RT-PCR)

To confirm the microarray data, RNA was freshly isolated from nine of the pre-imatinib mesylate samples of the trial (Radiation Therapy Oncology Group 19, 22, 31, 39, 47, 56), including three samples (Radiation Therapy Oncology Group 25, 35, and 53) not included in the original microarray analyses and reverse transcribed to cDNA by SuperScript II reverse transcriptase (Invitrogen). Expression of RNA for three *KRAB-ZNF* genes (ZNF 91, ZNF 43, and ZNF 208) and two endogenous control genes (HPRT and 18S) was measured in each presample by real-time PCR (with TaqMan Gene Expression Assay products on an ABI PRISM 7900 HT Sequence Detection System, Applied Biosystems), following protocols recommended by the manufacturer and as previously described (30). The relative mRNA expressions of ZNF 91, ZNF 43, and ZNF 208 were adjusted with either HPRT or 18S. The primer/probe fluorescein phosphoramidite (FAM) sets for ZNF 91, ZNF 43, ZNF 208, HPRT, and 18S were obtained from Applied Biosystems.

siRNA Transfection and Imatinib Mesylate Sensitivity

Two siRNAs against each ZNF of interest (Qiagen) were pooled together, and GIST cells were reverse transfected in four 96-well plates, as described according to the protocols provided by the manufacturer (Qiagen). In addition, siRNA smart pools against KIT and GL-2 (Dharmacon) were used as positive and negative controls, respectively, and used for Z-score calculations. Forty-eight hours later, vehicle only or vehicle + imatinib mesylate (45 nmol/L) were added to two plates. After, 24-h cell viability was assessed using the cell titer blue assay. This assay is based on the ability of living cells to convert the redox dye, resazurin, into the fluorescent end product, resorufin. Cell titer blue was added to all wells and incubated for 4 h followed by data recording using an EnVision microplate reader (PerkinElmer).

Results

Radiation Therapy Oncology Group S0132 Trial Design and Patient Response to Imatinib Mesylate

Sixty-three patients with primary or recurrent potentially resectable malignant GIST from 18 institutions were originally enrolled onto the trial beginning in February 2002 and ending in June 2006 (15). A tumor positive for KIT (CD117) staining by IHC was the necessary prerequisite for patient enrollment. Fifty-three percent of primary tumors were located in the stomach, 27% in small bowel, and 20% in other sites within the gastrointestinal tract. Metastatic tumors were primarily located in the abdomen/peritoneum. Additional clinical information is shown in Table 1. Before the start of the 8 to 12 week imatinib mesylate regimen, a CT scan was done, and a tumor biopsy (pretreatment sample) was obtained. CT scans were repeated ~4 to 6 weeks into imatinib mesylate therapy and again immediately before surgical resection (after 8–12 weeks imatinib mesylate therapy; Fig. 1A). CT measurements, taken from the longest cross-sectional diameter of the primary GIST or the index metastatic lesion(s), were used to assess tumor response (i.e. tumor shrinkage, no measurable change, or tumor enlargement) to imatinib mesylate therapy (Fig. 1B). Of the 52 analyzable patients, 58% (30 of 52) had surgical resection of primary locally advanced GIST, whereas 42% (22 of 52) had recurrent/metastatic GIST resected. Genomic DNA was isolated from available large biopsies (pretreatment samples) or resected tumor (posttreatment samples), and *KIT* and

PDGFRA mutational analysis was done (Fig. 1B). Mutational analysis was done on 39 of the 52 patients, and the most frequent mutations occurred in exon 11 (82%, 32 of 39), followed by exon 9 (3%, 1 of 39). No mutations were found in exons 13 and 17 of *KIT* or in exons 12, 14, and 18 of *PDGFRA*. Fifteen percent (6 of 39) of the patients tested lacked mutations in *KIT* and *PDGFRA*. Similar frequencies have been observed previously (12).

Gene Expression Profiles Associated with Response to Imatinib Mesylate

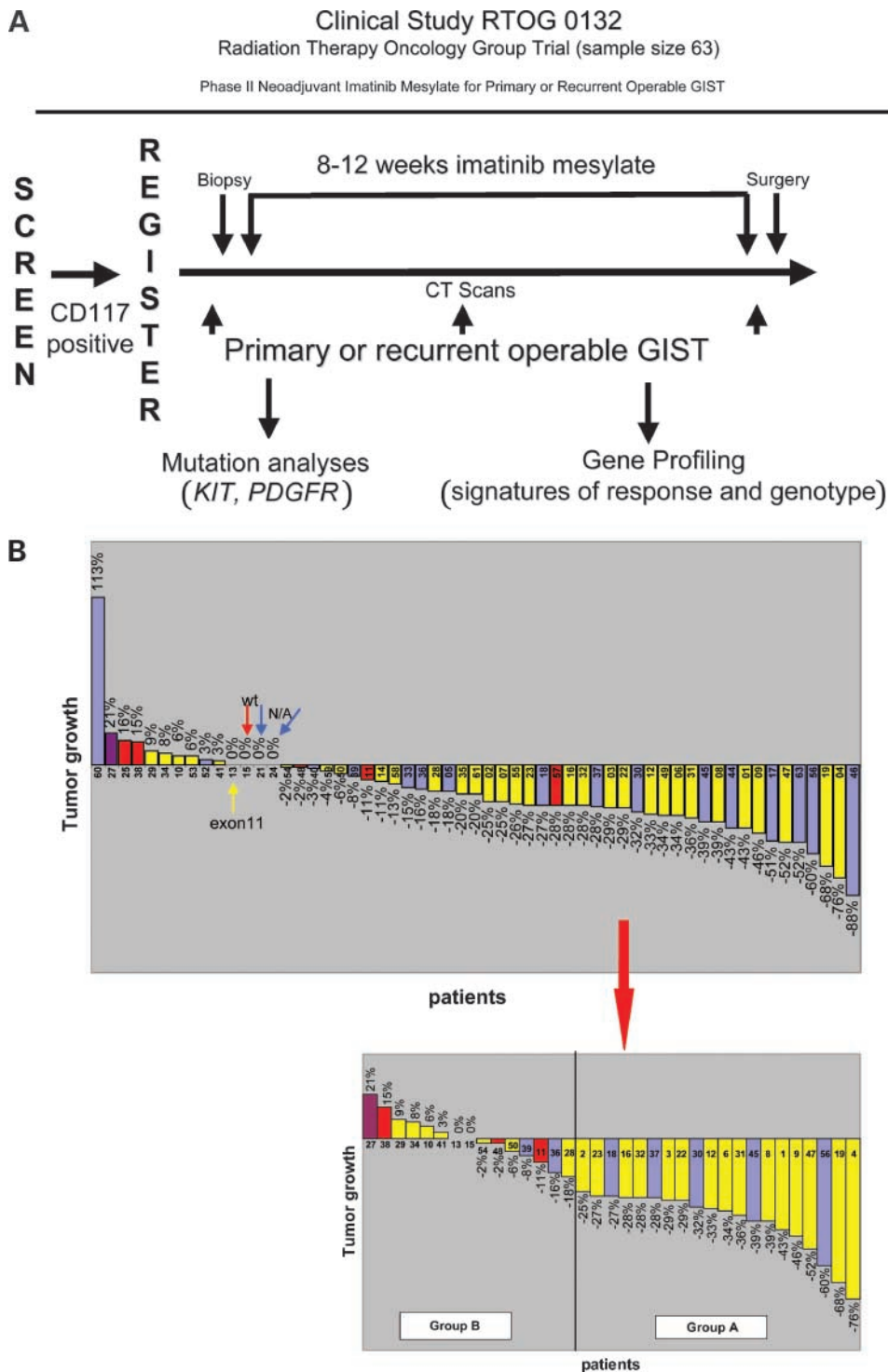
RNA was isolated from both pre- and posttreatment samples, and those deemed of adequate amount and quality were evaluated by using Agilent oligonucleotide microarrays (see Methods). GIST specimens (pre, post, or both) used for microarray analysis are shown in Fig. 1B (bottom). CT measurements were used to classify patients as either "immediate responders" (group A) if the patient's tumor showed a $\geq 25\%$ reduction in size during the 8 to 12 weeks of imatinib mesylate treatment. The other GIST samples were combined and will subsequently be referred to as group B. The index used for these latter tumors ranged from an 18% diameter reduction to a 21% tumor enlargement after 8 to 12 weeks of imatinib mesylate. Mutation status alone was not a sole predictor of response to short-term imatinib mesylate treatment. Seventy-five percent (15 of 20) of biopsy samples from group A possessed an exon 11 *KIT* mutation. The remaining 25% (5 of 20) had no mutational analysis available. In comparison, 53% (8 of 15) of samples from group B had exon 11 *KIT* mutations, whereas the remaining samples possessed an exon 9 *KIT* mutant (7%, 1 of 15), were *KIT*/*PDGFRA* mutation negative (27%, 4 of 15), or were undetermined (13%, 2 of 15). Using the array data generated from the pretreatment biopsy specimen RNAs, Statistical Analysis of Microarrays identified 38 genes as differentially expressed at a false discovery rate of 10% between the two groups, with all gene transcripts present at higher levels in patients within group B (Table 2). Thirty-two of these corresponded to known genes; 18 of these are *KRAB-ZNF* genes, 10 of which mapped to the same locus (*HSA19p12-19p13.1*). Two additional genes, *LOC646825* and *LOC388523*, showed similarity to *ZNF 91* and *ZNF 208* (Fig. 2). Other genes within this signature encode for the ZNF-containing proteins *ZMYND11* and *ZMAT1* and transcription factors *GTF2I* and *GABPAP*. The remaining genes encode the following proteins: *RASSF8*, *WDR90*, *SF3B1*, *UGT2B7*, and four hypothetical proteins (Table 2).

The observation that most genes within this predictive signature were *KRAB-ZNF* genes (18 of 32), 10 of which are located within the same chromosomal region (*HSA19p12-19p13.1*), was intriguing and warranted further study. Analysis of pretreatment sample expression differences for all genes within the *19p12-13.1* locus showed a consistent difference (Fig. 3A, red box). All the *ZNF* genes showed higher overall expression in samples from patients within group B across the locus, although adjoining genes showed equal expression between the two groups. Of additional interest, these *KRAB-ZNFs* seem to be coordinately

Table 1. Characteristics of patients and tumors

	n (%)
Median age (range), y	58.5 (24 to 84)
Sex	
Female	24 (46)
Male	8 (54)
Primary tumor	30 (58)
Metastatic/recurrent tumor	22 (42)
Site of primary tumor	
Stomach	16 (53)
Small bowel	8 (27)
Other	6 (20)
Site of metastatic tumor	
Abdomen/peritoneum	15 (68)
Liver only	6 (27)
Liver/peritoneum	1 (5)
Size of tumor, cm	
≤ 10	37 (71)
> 10	15 (29)
Mutation	
Exon 11 <i>KIT</i>	32 (62)
Exon 9 <i>KIT</i>	1 (2)
Exon 17 <i>KIT</i>	0 (0)
<i>PDGFRA</i> (exons 18 and 12)	0 (0)
Wild type	6 (12)
N/A*	13 (25)

*N/A, not applicable, not enough tissue for mutational analysis.



regulated in response to imatinib mesylate therapy in that KRAB-ZNF mRNA levels decrease in tumors from patients in group B after imatinib mesylate. To rule out the possibility that an enrichment of other nontumor cells, such as endothelial and inflammatory cells, may be contributing to the observed expression patterns, we examined the cel-

lular content of the post-imatinib mesylate samples and used only those that displayed $> 70\%$ tumor cellularity (Fig. 3B). We also observed a very similar pattern of decreased ZNF expression in the group B post-imatinib mesylate samples with lower tumor ($< 70\%$) cellularity (data not shown), suggesting that the observed trend is likely

associated with tumor cell response to imatinib mesylate. Analysis of the pre- and posttreatment samples from group A showed an opposing trend in that the level of ZNF genes increased following the 8 to 12 week imatinib mesylate regimen; however, because the cellularity was <70% for all but one of these samples, we cannot rule out the effect of nontumor cells on these expression patterns (data not shown).

Validation with Quantitative RT-PCR

We used quantitative RT-PCR to validate the differential expression pattern of the predictor genes. For this analysis, four genes were selected from the list of 18 KRAB-ZNF genes identified in the microarray analysis based on availability of commercial quantitative RT-PCR assays. We found the assays for ZNF 43, ZNF 208, and ZNF 91 to

work reliably. All three were expressed significantly higher in group B before imatinib mesylate treatment compared with the immediate response group. The expression of each gene was evaluated in a small validation panel consisting of nine pretreatment samples from patients on the trial for which high quality RNAs could be isolated (see Methods). ZNF 43, ZNF 208, and ZNF 91 mRNA levels were significantly lower in patients whose tumors rapidly shrunk in response to imatinib mesylate than in those who did not (Fig. 4). Expression levels of the three genes were highly correlated with each other (all pairwise correlations were >0.93 with P s < 0.0003).

We next sought to determine if modifying the expression of a subset of the genes within this predictive signature could alter the sensitivity of GIST cells to imatinib mesylate.

Table 2. Significance analysis of microarrays analysis of genes differentially expressed between rapid responders and stable disease

Accession	Gene symbol	Description	Cytoband	SAM score
NM_178549	ZNF678	ZNF protein 678	1q42.13	4.10
NM_212479	ZMYND11	ZNF, MYND domain containing 11	10p15.3	4.11
NM_007211	RASSF8	Ras association (RalGDS/AF-6) domain family 8	12p12.1	3.55
A_24_P75888	N/A	N/A	14q11.1	4.35
AK126622	WDR90	WD repeat domain 90	16p13.3	3.61
A_24_P717262	N/A	N/A	19p12	4.23
ENST00000341262	ZNF56	ZNF protein 56 (fragment)	19p12	3.97
AK131420	ZNF66	ZNF protein 66	19p12	4.06
NM_003429	ZNF85	ZNF protein 85	19p12	4.36
NM_133473	ZNF431	ZNF protein 431	19p12	3.90
NM_001001415	ZNF429	ZNF protein 429	19p12	4.29
NM_003423	ZNF43	ZNF protein 43	19p12	4.10
NM_007153	ZNF208	ZNF protein 208	19p12	3.69
NM_001001411	ZNF676	ZNF protein 676	19p12	4.08
ENST00000357491	LOC646825	Discontinued, similar to ZNF protein 91	19p12	4.14
NM_001080409	ZNF99	ZNF protein 99	19p12	3.84
XR_017338	LOC388523	Similar to ZNF protein 208	19p12	4.10
NM_003430	ZNF91	ZNF protein 91	19p12	3.95
ENST00000334564	ZNF528	ZNF protein 528	19q13.33	3.92
NM_024733	ZNF665	ZNF protein 665	19q13.41	3.74
NM_001004301	ZNF813	ZNF protein 813	19q13.41	3.86
AK001808	N/A	CDNA FLJ10946 fis, clone PLACE1000005	2q24.3	4.21
BE168511	SF3B1	Splicing factor 3b, subunit 1, 155kDa	2q33.1	3.86
NM_138402	LOC93349	Hypothetical protein BC004921	2q37.1	4.42
ENST00000305570	LOC727867	Similar to PRED65	21q11.2	3.57
ENST00000341087	N/A	N/A	4p16.3	4.53
NM_001074	UGT2B7	UDP glucuronosyltransferase 2 family, polypeptide B7	4q13.2	3.66
NM_182524	ZNF595	ZNF protein 595	4p16.3	3.71
THC2708803	N/A	N/A	4q22.3	3.85
A_24_P492885	N/A	N/A	7q11.21	4.39
XM_001127354	LOC728376	Similar to hCG1996858	7p11.2	4.48
AF277624	ZNF479	ZNF protein 479	7p11.2	4.19
NR_002723	GABPAP	GA binding protein TF, α subunit pseudogene	7q11.21	4.14
XM_001128828	LOC728927	Similar to hCG40110	7q11.21	4.05
NM_178558	ZNF680	ZNF protein 680	7q11.21	3.59
NM_001518	GTF2I	General TF II, i	7q11.23	4.09
NM_197977	ZNF189	ZNF protein 189	9q31.1	3.64
NM_032441	ZMAT1	ZNF, matrin type 1	Xq22.1	3.74

Abbreviations: SAM, Statistical Analysis of Microarrays; TF, transcription factor.

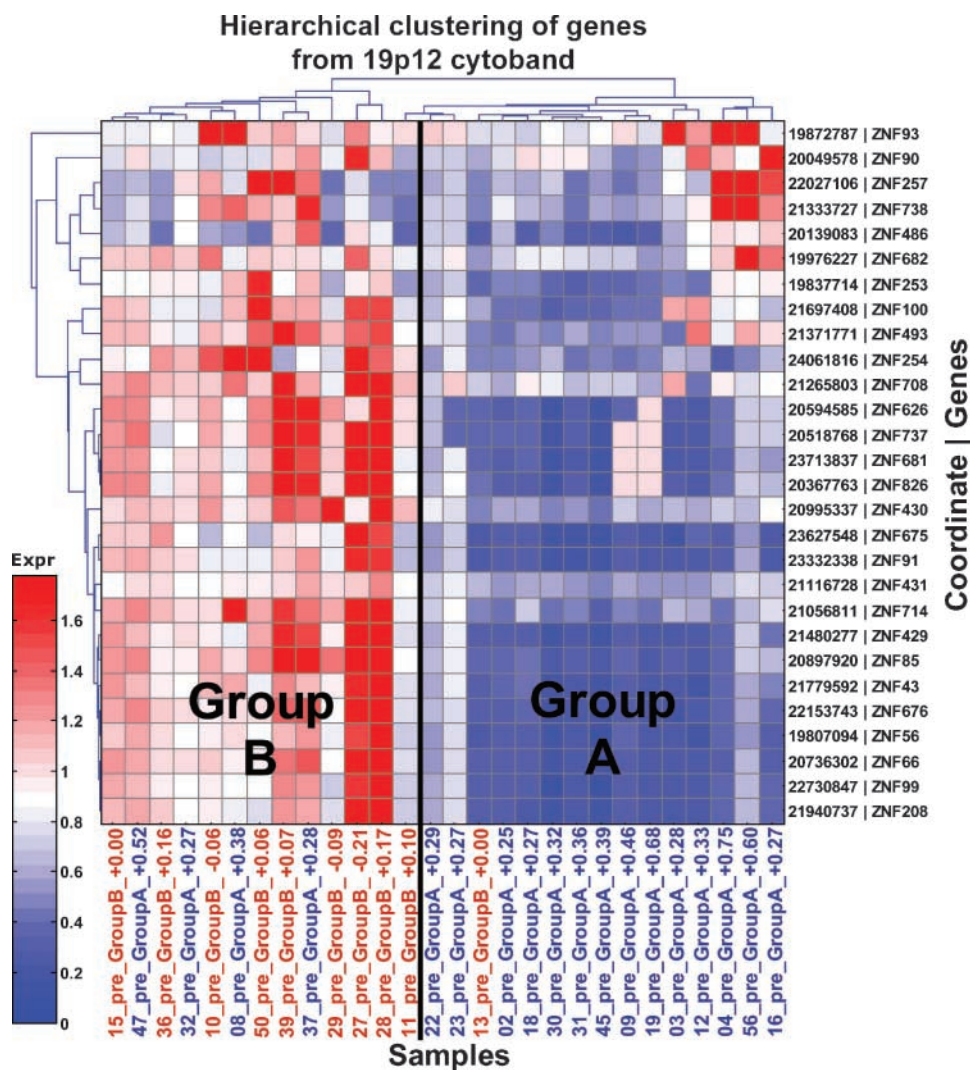


Figure 2. Gene expression profiles associated with response to imatinib mesylate. A heat map showing the HSA19p12-13.1 KRAB-ZNF hierarchical cluster. In the image, blue is down-regulation, whereas red is up-regulation. Patients who initially responded rapidly to imatinib mesylate clearly show decreased KRAB-ZNF expression compared with the others.

We selected ZNF 208, ZNF 91, ZNF 85, and ZNF 43 for siRNA targeted knockdown. From these screens, we showed that depletion of each of the four ZNFs were able to sensitize GIST cells to varying degrees of imatinib mesylate (sensitization index, viability with drug/viability with vehicle only was 0.58 to 0.85). These findings suggest that some members of this gene signature may not only have predictive value but functional relevance to imatinib mesylate activity *in vivo*. We also developed genomic-based quantitative PCR analysis to assess gene copy number of these KRAB-ZNF genes. We found that up-regulation of these ZNFs in patients within group B was not associated with gene amplification (data not shown), indicating that the changes in mRNA were independent of gene copy number.

Discussion

In this study, we set out to obtain a gene expression profile that could be predictive of likely imatinib mesylate-induced

cytoreduction in GIST patients before therapy. Because several alternative options for progressive disease treatment are currently being evaluated, such as new kinase inhibitors or combination therapy with imatinib mesylate, such a profile may be useful in determining appropriate personalized clinical treatment of GIST patients.

The clinical trial from which tissue samples were obtained for this study has yielded some interesting findings. Most patients on this trial had apparent clinical benefit from imatinib mesylate therapy before surgery. Forty-nine percent of all patients enrolled onto the trial manifested $\geq 25\%$ tumor size reduction following the initiation of 8 to 12 weeks of imatinib mesylate therapy, with 75.4% having at least some degree of tumor response (Fig. 1B). In addition, preoperative imatinib mesylate therapy was associated with minimal drug related toxicity and surgical morbidity (31). We observed benefit from the neoadjuvant use of imatinib mesylate for downsizing tumors before surgical resection. Using pre-imatinib mesylate samples from this study, microarray

analyses were done to obtain a gene expression profile that may be indicative of the likely response to short-term imatinib mesylate therapy. Although expression of several interesting genes, such as *RASSF8*, *SF3B1*, and *UGT2B7*, were

found to be associated with differential response to imatinib mesylate, we were drawn to the observation that nearly a third of the genes clustered in one locus on chromosome 19p12 near the centromere (Fig. 2). These differentially

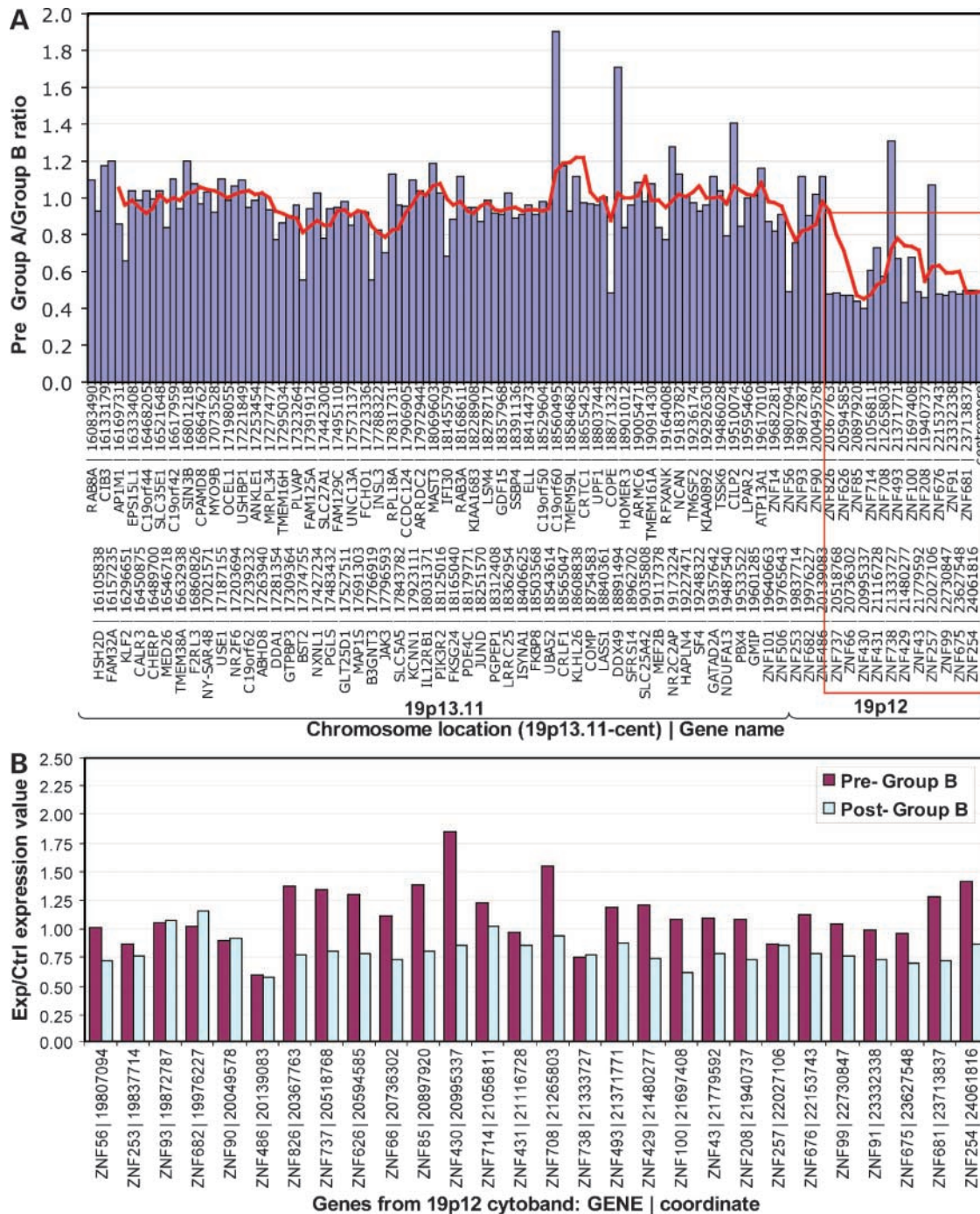


Figure 3. *KRAB-ZNF* gene expression on chromosome 19p12-13.1 before and after imatinib mesylate therapy. **A**, analysis of pretreatment ratios of tumors showing >25% (group A) or <25% reduction (group B) using data from 28 patients for all genes in the 19p12-13.1 locus. All gene symbols and locations are shown stepwise. All genes in this locus (red box) showed higher mean ZNF expression levels in group B samples (i.e., lower group A/group B ratio), whereas adjoining genes showed roughly equal expression between the two groups. **B**, analysis of changes in expression of genes in this locus upon imatinib mesylate treatment in group B samples with >70% tumor cellularity. Red columns, means of pretreatment samples from group B; blue columns, means of posttreatment samples from group B.

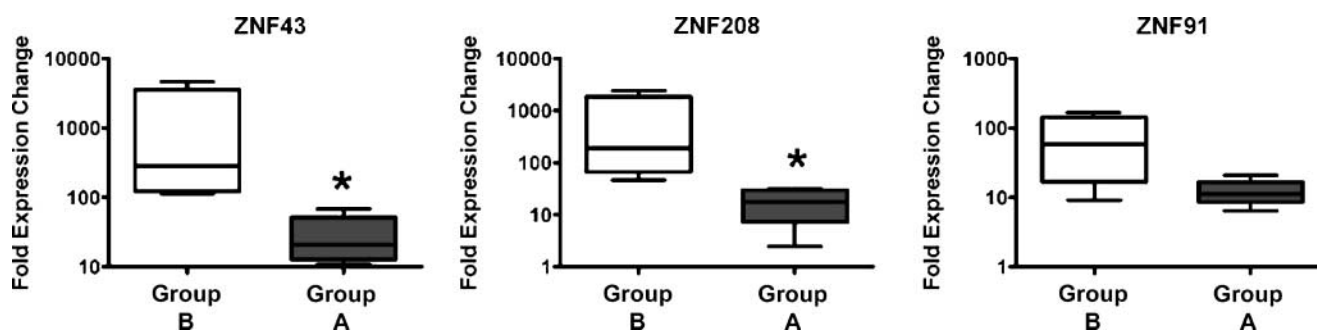


Figure 4. Validation of *ZNF* gene expression by quantitative RT-PCR. Fold expression changes of three of the *ZNF*s within the predictive signature gene panel, that is, ZNF 43, ZNF 208, and ZNF 91, were measured using quantitative RT-PCR. The ratios of each gene to control (HPRT or actin) were measured using total RNAs from nine pretreatment samples (five in group A and four in group B) and universal human reference RNA. The relative median mRNA levels for ZNF 43, ZNF 208, and ZNF 91 in group A were 412-, 257-, and 77-fold higher as compared with controls, whereas the median levels in group B were 21-, 18-, and 11-fold normalized to controls, respectively. Two-sided Wilcoxon rank sum tests were used to compare the distribution of ZNF 43, ZNF 208, and ZNF 91 mRNA expression between the two groups, and Pearson's coefficients were used to measure the pairwise correlation of the *ZNF* gene expression. Tests were conducted using a 5% type I error. The predictive value of ZNF 43 and ZNF 208 were found to be statistically significant. *, $P = 0.02$. Results are of three independent experiments.

expressed *ZNF*s are *KRAB-ZNF* genes that are members of the ZNF 91 subfamily (32, 33). In addition, we showed that expression of these *ZNF*s seemed to be coordinately regulated by imatinib mesylate treatment (Fig. 3B and data not shown).

The ZNF 91 subfamily includes 64 genes, 37 of which are found on chromosome 19 (32). These *KRAB-ZNF* proteins are characterized by the presence of a DNA-binding domain composed of between 4 and 30 ZNF motifs and a *KRAB* domain near the amino terminus. They form one of the largest families of transcriptional regulators. Many members of this family are still uncharacterized, and the specific functions of many members are unknown; however, some of these *ZNF*s have been associated with undifferentiated cells and also implicated in cancers. Lovering and Trowsdale (34) showed that expression of ZNF 43 was increased in lymphoid cell lines and that inducing terminal differentiation *in vitro* in one of these cell lines led to reduced ZNF 43 expression. Another study using microarrays comparing normal controls to mononuclear cells of acute myelogenous leukemia patients showed ZNF 91 expression was increased in 93% of acute myelogenous leukemia cases and that inhibiting expression of ZNF 91 induced apoptosis of these cells (35). Eight other *ZNF*s, not found to reach significance in our tests for differential expression in our studies, have been denoted as "candidate cancer genes" or *CAN* genes by large-scale mutagenesis screens in breast and colorectal cancers (36).

In addition, *KRAB-ZNF* expression has been associated with resistance to imatinib mesylate. Using DNA microarrays, Chung et al. (37) showed that 22 genes, two of which are *ZNF*s, were positively correlated with increasing imatinib mesylate dosage in chronic myelogenous leukemia cell lines. Therefore, our study is not the first to link response to imatinib mesylate with *KRAB-ZNF* expression but is the first to establish this connection in GIST patients and to the genes within the *HSA19p12-19p13.1* locus. The ultimate goal of this work was to identify a profile that is indicative

of immediate response to imatinib mesylate so that, in the future, expression of these *ZNF*s can be examined in patient biopsies before treatment, allowing for the most effective therapeutic regimen to be used, particularly in relation to planned surgical resection. Because there is significant overexpression of these *KRAB-ZNF*s and other genes within the predictive signature in patients who are not as responsive to imatinib mesylate, our study suggests that IHC-based or quantitative RT-PCR expression analyses of these genes could potentially serve as a rapid means for prescreening GIST patients before treatment. However, it should be reiterated that this predictive gene signature was established using a 25% decrease in tumor size cutoff for response rather than RECIST or Choi criteria because this was a neoadjuvant trial and the design of the trial (8–12 weeks of imatinib) was not to assess short-term imatinib response by standard criteria. Nevertheless, it will be important to further evaluate these predictive biomarkers using independent cohorts of GIST samples with clinical outcome information.

We have shown that quantitative RT-PCR assays are informative when adequate RNA samples can be obtained either from small needle biopsies or resected tumor samples. Our studies also highlight the need for additional studies to assess the role of these *KRAB-ZNF*s in potentially mediating imatinib mesylate response. In preliminary studies, we have found that siRNA-mediated targeted knockdown of ZNF 208, ZNF 91, ZNF 85, and ZNF 43 can enhance the sensitivity of GIST cells to imatinib mesylate, albeit to varying degrees. Further functional studies are currently underway to determine how these genes may be influencing imatinib mesylate activity in GISTs and their potential clinical therapeutic value.

We also searched for links about why many of these *ZNF* genes within a single locus are coordinately regulated at the expression level. Using transcription factor binding site analysis from advanced biomedical computing center and viewed using CIMminer software, we sought to identify

common transcription factors that could explain why, in some samples, all the genes are either up-regulated or down-regulated. The analysis showed that there are a number of transcription factors that regulate these ZNFs (data not shown). One transcription factor, HinfA, seemed to be associated with 12 of the ZNFs of interest. HinfA is a transcription factor known to bind to A/T-rich repeats in the promoters of human histone (*H3* and *H4*) genes (38). However, HinfA was not measured on our array. Vogel et al. (39) have found that the heterochromatin binding proteins, CBX1 and SUV39H1, have been associated with coexpression of *ZNF* genes. However, our analysis of the three probes for CBX1 and one probe for SUV39H1 did not detect significant differences in expression between these two groups.

In summary, we were able to elucidate a gene expression profile that is unique to patients whose tumors are less responsive to imatinib mesylate in comparison with those that rapidly respond. This profile consists of 38 genes (32 annotated), 18 of which are KRAB-ZNFs. We feel that these results have potential clinical relevance and could help stratify patients most responsive to imatinib mesylate and potentially design more effective treatment regimens particularly in neoadjuvant use for GIST patients in the future.

Disclosure of Potential Conflicts of Interest

No potential conflicts of interest were disclosed.

Acknowledgments

We thank the valuable input of Drs. Chi Tarn, Chong Xu, Harsh Pathak, Yan Zhou, and Eric Ross on this manuscript; Lisa Vanderveer for the technical support; the Biosample Repository Core Facility, the Clinical Molecular Genetics Laboratory, and the Genome Core Facility at Fox Chase Cancer Center, and the Radiation Therapy Oncology Group Tissue Bank for the tissue studies; and Tania Stutman and the Gastrointestinal Stromal Tumor Cancer Research Fund for providing a fellowship to L. Rink.

References

- Corless CL, Heinrich MC. Molecular pathobiology of gastrointestinal stromal sarcomas. *Ann Rev Pathol* 2008;3:557–86.
- El-Rifai W, Sarlomo-Rikala M, Andersson LC, Knuutila S, Miettinen M. DNA sequence copy number changes in gastrointestinal stromal tumors: tumor progression and prognostic significance. *Cancer Res* 2000;60:3899–903.
- Miettinen M, Lasota J. Gastrointestinal stromal tumors: review on morphology, molecular pathology, prognosis, and differential diagnosis. *Archiv Pathol Lab Med* 2006;130:1466–78.
- Tworek JA, Appelman HD, Singleton TP, Greenson JK. Stromal tumors of the jejunum and ileum. *Mod Pathol* 1997;10:200–9.
- Miettinen M, Kopczynski J, Makhlof HR, et al. Gastrointestinal stromal tumors, intramural leiomyomas, and leiomyosarcomas in the duodenum: a clinicopathologic, immunohistochemical, and molecular genetic study of 167 cases. *Am J Surg Pathol* 2003;27:625–41.
- Tworek JA, Goldblum JR, Weiss SW, Greenson JK, Appelman HD. Stromal tumors of the anorectum: a clinicopathologic study of 22 cases. *Am J Surg Pathol* 1999;23:946–54.
- Miettinen M, Monihan JM, Sarlomo-Rikala M, et al. Gastrointestinal stromal tumors/smooth muscle tumors (GISTs) primary in the omentum and mesentery: clinicopathologic and immunohistochemical study of 26 cases. *Am J Surg Pathol* 1999;23:1109–18.
- Corless CL, Fletcher JA, Heinrich MC. Biology of gastrointestinal stromal tumors. *J Clin Oncol* 2004;22:3813–25.
- Mazur MT, Clark HB. Gastric stromal tumors. Reappraisal of histogenesis. *Am J Surg Pathol* 1983;7:507–19.
- Graadt van Roggen JF, van Velthuysen ML, Hogendoorn PC. The histopathological differential diagnosis of gastrointestinal stromal tumours. *J Clin Pathol* 2001;54:96–102.
- Heinrich MC, Corless CL. Gastric GI stromal tumors (GISTs): the role of surgery in the era of targeted therapy. *J Surg Oncol* 2005;90:195–207, discussion.
- Subramanian S, West RB, Corless CL, et al. Gastrointestinal stromal tumors (GISTs) with KIT and PDGFRA mutations have distinct gene expression profiles. *Oncogene* 2004;23:7780–90.
- Tarn C, Merkel E, Canutescu AA, et al. Analysis of KIT mutations in sporadic and familial gastrointestinal stromal tumors: therapeutic implications through protein modeling. *Clin Cancer Res* 2005;11:3668–77.
- Debiec-Rychter M, Sciot R, Le Cesne A, et al. KIT mutations and dose selection for imatinib in patients with advanced gastrointestinal stromal tumours. *Eur J Cancer* 2006;42:1093–103.
- Eisenberg BL, Judson I. Surgery and imatinib in the management of GIST: emerging approaches to adjuvant and neoadjuvant therapy. *Ann Surg Oncol* 2004;11:465–75.
- DeMatteo RP, Lewis JJ, Leung D, Mudan SS, Woodruff JM, Brennan MF. Two hundred gastrointestinal stromal tumors: recurrence patterns and prognostic factors for survival. *Ann Surg* 2000;231:51–8.
- Demetri GD, von Mehren M, Blanke CD, et al. Efficacy and safety of imatinib mesylate in advanced gastrointestinal stromal tumors. *N Engl J Med* 2002;347:472–80.
- Verweij J, Casali PG, Zalcberg J, et al. Progression-free survival in gastrointestinal stromal tumours with high-dose imatinib: randomised trial. *Lancet* 2004;364:1127–34.
- Van den Abbeele AD, Badawi RD. Use of positron emission tomography in oncology and its potential role to assess response to imatinib mesylate therapy in gastrointestinal stromal tumors (GISTs). *Eur J Cancer* 2002;38 Suppl 5:S60–5.
- Zalcberg JR, Verweij J, Casali PG, et al. Outcome of patients with advanced gastro-intestinal stromal tumours crossing over to a daily imatinib dose of 800 mg after progression on 400 mg. *Eur J Cancer* 2005;41:1751–7.
- Prenen H, Cools J, Mentens N, et al. Efficacy of the kinase inhibitor SU11248 against gastrointestinal stromal tumor mutants refractory to imatinib mesylate. *Clin Cancer Res* 2006;12:2622–7.
- Weisberg E, Wright RD, Jiang J, et al. Effects of PKC412, nilotinib, and imatinib against GIST-associated PDGFRA mutants with differential imatinib sensitivity. *Gastroenterology* 2006;131:1734–42.
- Schittenhelm MM, Shiraga S, Schroeder A, et al. Dasatinib (BMS-354825), a dual SRC/ABL kinase inhibitor, inhibits the kinase activity of wild-type, juxtamembrane, and activation loop mutant KIT isoforms associated with human malignancies. *Cancer Res* 2006;66:473–81.
- Bauer S, Yu LK, Demetri GD, Fletcher JA. Heat shock protein 90 inhibition in imatinib-resistant gastrointestinal stromal tumor. *Cancer Res* 2006;66:9153–61.
- Godwin AK, Vanderveer L, Schultz DC, et al. A common region of deletion on chromosome 17q in both sporadic and familial epithelial ovarian tumors distal to BRCA1. *Am J Hum Genet* 1994;55:666–77.
- Corless CL, McGreevey L, Haley A, Town A, Heinrich MC. KIT mutations are common in incidental gastrointestinal stromal tumors one centimeter or less in size. *Am J Pathol* 2002;160:1567–72.
- Grant JD, Somers LA, Zhang Y, Manion FJ, Bidaut G, Ochs MF. FGDP: functional genomics data pipeline for automated, multiple microarray data analyses. *Bioinformatics (Oxford, England)* 2004;20:282–3.
- Tusher VG, Tibshirani R, Chu G. Significance analysis of microarrays applied to the ionizing radiation response. *Proc Natl Acad Sci U S A* 2001;98:5116–21.
- Saeed AI, Sharov V, White J, et al. TM4: a free, open-source system for microarray data management and analysis. *BioTechniques* 2003;34:374–8.
- Chen X, Arciero CA, Wang C, Broccoli D, Godwin AK. BRCC36 is essential for ionizing radiation-induced BRCA1 phosphorylation and nuclear foci formation. *Cancer Res* 2006;66:5039–46.
- Heinrich MC, Corless CL, Blanke CD, et al. Molecular correlates of

2182 Gene Signatures and Response to Imatinib Mesylate

- imatinib resistance in gastrointestinal stromal tumors. *J Clin Oncol* 2006;24:4764–74.
32. Hamilton AT, Huntley S, Tran-Gyamfi M, Baggott DM, Gordon L, Stubbs L. Evolutionary expansion and divergence in the ZNF91 subfamily of primate-specific zinc finger genes. *Genome Res* 2006;16:584–94.
33. Mark C, Abrink M, Hellman L. Comparative analysis of KRAB zinc finger proteins in rodents and man: evidence for several evolutionarily distinct subfamilies of KRAB zinc finger genes. *DNA Cell Biol* 1999;18:381–96.
34. Lovering R, Trowsdale J. A gene encoding 22 highly related zinc fingers is expressed in lymphoid cell lines. *Nucleic Acids Res* 1991;19:2921–8.
35. Unoki M, Okutsu J, Nakamura Y. Identification of a novel human gene, *ZFP91*, involved in acute myelogenous leukemia. *Int J Oncol* 2003;22:1217–23.
36. Sjoblom T, Jones S, Wood LD, et al. The consensus coding sequences of human breast and colorectal cancers. *Science (New York, NY)* 2006;314:268–74.
37. Chung YJ, Kim TM, Kim DW, et al. Gene expression signatures associated with the resistance to imatinib. *Leukemia* 2006;20:1542–50.
38. van Wijnen AJ, Massung RF, Stein JL, Stein GS. Human H1 histone gene promoter CCAAT box binding protein HiNF-B is a mosaic factor. *Biochemistry* 1988;27:6534–41.
39. Vogel MJ, Guelen L, de Wit E, et al. Human heterochromatin proteins form large domains containing *KRAB-ZNF* genes. *Genome Res* 2006;16:1493–504.

Molecular Cancer Therapeutics

Gene expression signatures and response to imatinib mesylate in gastrointestinal stromal tumor

Lori Rink, Yuliya Skorobogatko, Andrew V. Kossenkov, et al.

Mol Cancer Ther 2009;8:2172-2182. Published OnlineFirst August 11, 2009.

Updated version Access the most recent version of this article at:
doi:[10.1158/1535-7163.MCT-09-0193](https://doi.org/10.1158/1535-7163.MCT-09-0193)

Cited articles This article cites 39 articles, 12 of which you can access for free at:
<http://mct.aacrjournals.org/content/8/8/2172.full#ref-list-1>

Citing articles This article has been cited by 8 HighWire-hosted articles. Access the articles at:
<http://mct.aacrjournals.org/content/8/8/2172.full#related-urls>

E-mail alerts [Sign up to receive free email-alerts](#) related to this article or journal.

Reprints and Subscriptions To order reprints of this article or to subscribe to the journal, contact the AACR Publications Department at pubs@aacr.org.

Permissions To request permission to re-use all or part of this article, use this link
<http://mct.aacrjournals.org/content/8/8/2172>.
Click on "Request Permissions" which will take you to the Copyright Clearance Center's (CCC) Rightslink site.